



Effect of tannic acid on properties of electrospun gelatin nanofibres

Abolfazl Mozaffari¹, Mohammad Mirjalili^{1,a}, Mazeyar Parvinzadeh Gashti² & Masoud Parsania³

¹Department of Textile Engineering, Yazd Branch, Islamic Azad University, Yazd, Iran

²Research and Development Laboratory, PRE Labs Inc., 3302 Appaloosa Road, Unit 3, Kelowna, British Columbia, Canada

³Department of Microbiology, Faculty of Medicine, Tehran Medical Sciences, Islamic Azad University, Tehran

Received 6 October 2018; revised received and accepted 29 January 2019

Gelatin/tannic acid nanofibres have been prepared and the effects of production parameters, including high voltage, feeding rate and distance between tip of the needle and collector on the morphology of nanofibres are investigated. The results show that the average nanofibre diameter increases with raising the high voltage values, due to less branching of liquid jet. Increasing the feeding rate leads to an increase in the nanofibre diameter, up to a certain value (0.6-0.8 mL/h). Further increase in the feeding rate value causes the formation of a ribbon-like structure. The increment in the content of tannic acid as a crosslinker increases the viscosity of the spinning solution and the average nanofibre diameters. Also, the tensile strength of crosslinked nanofibres increases as compared to that of the gelatin nanofibres. Moreover, the addition of tannic acid to gelatin nanofibres significantly enhances the antibacterial property of nanofibres.

Keywords: Crosslinking, Electrospinning, Gelatin scaffold, Tannic acid, Nanofibres

1 Introduction

Biodegradable synthetic polymer materials, such as poly (glycolic acid), poly (lactic acid) and their copolymers, poly (p-dioxanone), copolymers of trimethylene carbonate and glycolide have been used in a number of clinical applications. Most natural biodegradable polymer materials are derived from proteins, such as collagen, gelatin, and albumin, as well as polysaccharides, such as cellulose, hyaluronate, chitin and alginate. These polymer materials are different in their molecular weight, polydispersity, crystallinity, thermal transition, and degradation rate, which strongly affect polymer scaffold properties^{1,2}.

Polymeric scaffolds promote cell adhesion as well as maintenance of differentiated, cell function and direct the growth of cells³. However, cell affinity towards synthetic polymers is poor. Hence, many polymers, such as collagen, gelatin, alginate, chitosan, and hyaluronic acid are used for tissue engineering scaffolds⁴. Gelatin is a natural polymer with strong polarity. It has molecular chains connected through strong hydrogen bonds, constituting a 3D macromolecular network (double or triple helix) with reduced mobility^{5,6}. Because of

its various merits, such as biological origin, biodegradability, biocompatibility and commercial availability at relatively low cost, gelatin has been widely used in pharmaceutical and medical fields^{7,8}. One of the main reasons for using gelatin compared to collagen is that the triple helical structure is broken, and thus the R-G-D sequence is much better exposed, which may somehow be hidden in the collagen triple helical structure^{9,10}. In previous studies, scaffolds including gelatin were prepared to obtain desired porosity and biocompatibility for wound healing, drug release, tissue engineering or artificial skin engineering¹¹⁻¹³. However, these nanofibres are water soluble and have weak mechanical strength¹⁴. In this regard, crosslinking of gelatin nanofibres is carried out by glutaraldehyde, genipin and UV radiation^{14,15}.

Electrospinning is a simple and versatile technique to generate nano and micrometer fibrous structures which are very similar to the natural fibril extracellular matrix¹⁶⁻¹⁸. The morphology of electrospun fibres depends on the solution, device and environmental parameters^{19,20}. A great number of studies have been devoted to electrospinning of gelatin to produce nanofibres⁹. They influence of the process parameters on the properties of electrospun gelatin. They found that zeta potential and the

^a Corresponding author.
E-mail: dr.mirjalili@iauyazd.ac.ir

diffusion coefficients were higher in the case of dispersion electrospun gelatin than normal gelatin¹⁹. They used different organic solvents, including 2,2,2 trifluoro ethanol, to produce gelatin nanofibres. Their study showed that the PCL/gelatin nanofibres were produced with the diameter in the range of 100-340 nm (ref.21). Zhang *et al.*²² used formic acid as the solvent for electrospinning of gelatin and produced nanofibres with the diameter in the range of 70-170 nm. Moreover, some researchers have blended gelatin with other polymers and evaluated the spinning ability of blended nanofibres. Chong *et al.*²¹ produced nanofibres composites of gelatin/poly caprolactone. The produced nanofibres showed improved mechanical properties in comparison with pure gelatin. Ghasemi-Mobarakeh³ also used PCL/gelatin nanofibres scaffold for nerve tissue engineering.

An ideal bio-based crosslinking agent should be not only free from cytotoxicity but also have low cost. Such compound is capable of improving the mechanical performance of the materials in tissue engineering scaffolds^{23,24}. Tannic acid (TA) is d-glucose gallic acid ester containing multiple phenolic hydroxyl groups and aromatic rings. It is widely found in fruits, seeds of leguminous plants, grains and a variety of drinks (such as wine, tea, cocoa and apple juice). TA has a relatively high molecular weight and can interact with carbohydrate, proteins and other biological macromolecules^{23,25-27}. It is reported that tannic acid has bacteriostatic activity against food borne pathogens and that it is also known as an effective antioxidant²⁸. A review of related literature showed that none of the recent research studies has focused on the use of tannic acid as an antibacterial agent for crosslinking the gelatin nanofibres. Also, the effect of electrospinning parameters on the morphology and physical properties of gelatin/tannic acid nanofibres were not investigated. In this paper, tannic acid as an antioxidant and bio-friendly compound has been used for crosslinking the gelatin nanofibres, and the chemical and physical changes, which occurred after the crosslinking, are evaluated.

2 Materials and Methods

2.1 Materials

Gelatin powder (type A, Bio-Reagent with code G1890 from porcine skin), tannic acid and acetic acid (66%) were purchased from Sigma-Aldrich and deionized distilled water from Hydro Pars Kimia of Iran.

2.2 Preparation of Gelatin Nanofibres

According to the previous studies, acetic acid is commonly used as the solvent for electrospinning the gelatin. As a result of using acetic acid, the decomposition process slows down the polymer structure; the viscosity of the polymer solution increases to prevent the bead-like and uneven structure gelatin nanofibres¹. The spinning solution with the concentration of 20% w/w was prepared by dissolving 2 g gelatin in 5 mL acetic acid and 5 mL deionized distilled water. The electrospinning process was conducted at different high voltage values (15-25 kV), distances of the tip of needle to collector (12 cm and 15 cm) and feeding rates (0.4, 0.6, 0.8 and 1.0 mL/h). The electrospinning apparatus was acquired from Fanavaran Nano-Meghyas Co. (Iran), and nanofibres were collected onto aluminum (Al) sheet. The prepared nanofibres were placed in a vacuum oven at 45°C for 3 h to obtain a fully crosslinked structure.

2.3 Preparation of Gelatin/Tannic Acid Nanofibres and Crosslinking Strategies

For the crosslinked nanofibres, the solutions with the concentration of 15% w/v were prepared, and the tannic acid with the concentration of 3% and 5% w/w was added to the gelatin solution. The solutions were stirred at 30°C for 4h to obtain a homogenous solution.

2.4 Characterization

The morphology of gelatin nanofibres was studied by Scanning Electron Microscope (SEM, LEO1455VP, England). The average diameter of various nanofibres was determined by an image processor (SXM-196X). The FTIR spectra of nanofibres were examined by the FTIR spectroscopy (Thermo Nicolet NEXUS 870 FTIR from Nicolet Instrument Corp., USA). Thermogravimetric analysis of the scaffolds was carried out using a TG/DTA instrument (Pyris Diamond SII, Perkin Elmer Thermo Analyzer, USA) at the temperature range of 50–600 °C. The wettability of the scaffolds was investigated using a water contact angle system supported by videocam equipment (Perkin Elmer Spectrum RX-1, USA). The solubility of nanofibres was evaluated by immersing the nanofibres in a batch of distilled water for 120 min at 25°C and 7.4 pH. Afterwards, the nanofibres were dried at 40°C for 6 h. The samples were weighed and the solubility was calculated using the following equation:

$$\text{Solubility (\%)} = \frac{m_x - m_y}{m_y} \times 100 \quad \dots (1)$$

where m_x and m_y are the weights of nanofibres before and after the immersion in distilled water respectively.

Water absorbency measurement was performed via gravimetric analysis. 0.1 g of nanofibres was immersed in 50 mL of distilled water at 25°C for 120 min and 7.4 pH. Then, the weight of nanofibres was measured and the water absorbency (Q , g g⁻¹) was calculated as follows:

$$Q = \frac{m_a - m_b}{m_b} \quad \dots (2)$$

where m_b (g) and m_a (g) are the weights of the samples in the dry state and the swollen state at a certain time respectively²⁹.

The bacteriostatic test was performed by *S. aureus* (ATCC 25923) and *Escherichia coli* (ATCC 25922),

considering Gram-positive and Gram-negative bacteria respectively.

3 Results and Discussion

3.1 SEM Analysis

The characteristics of nanofibres can be adjusted by varying the electrospinning parameters. Among the various spinning parameters, viscosity, molecular weight of the polymer, applied voltage and distance from needle to collector are of great importance, affecting the nanofibre morphology directly²⁷.

The SEM images of gelatin nanofibres obtained at different spinning conditions are shown in Figs 1 (A-G). The results show that the nanofibre is not obtained at the gelatin concentration of 15% w/w, and many droplets are deposited on the collector (voltage 15-25 kV, feeding rate 0.8 mL/h and distance 15 cm). It seems that at the gelatin concentration of 15 %w/w, the effective entanglement of polymer chains does not occur, due to the far distances of the gelatin chains in the solution.

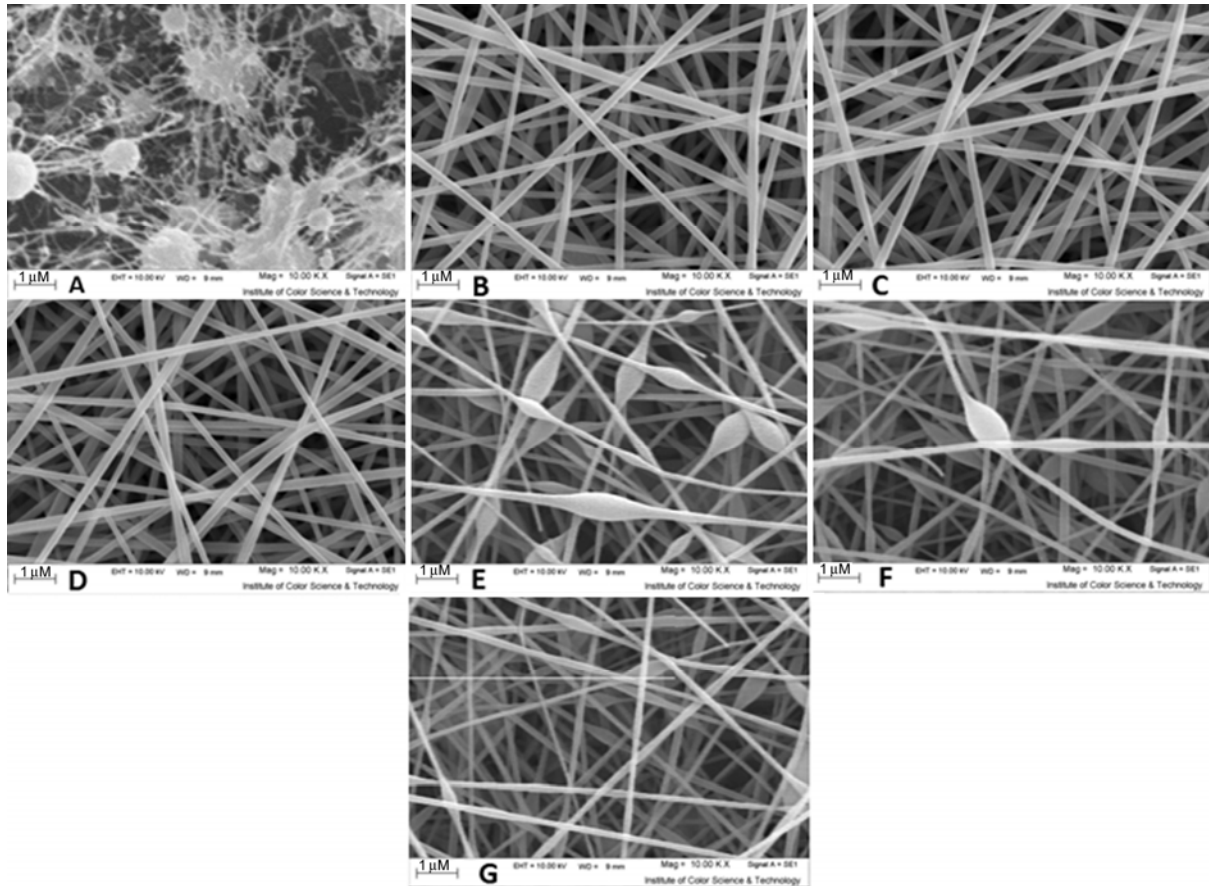


Fig. 1 — SEM images of (A) gelatin (15% w/w), 0.8 mL/h, 15 cm, 15-25 kV, (B) gelatin (20%w/w), 0.8 mL/h, 15 cm, 20-25 kV, (C) gelatin/tannic acid (15%/5% w/w), 0.8 mL/h, 15 cm, 20-25 kV, (D) gelatin/tannic acid (15%/3% w/w), 0.8 mL/h, 15 cm, 20-25 kV, (E) gelatin/tannic acid (20%/3%w/w), 0.8mL/h, 15cm, 20 kV, (F) gelatin/tannic acid (20%/3%w/w) 0.8mL/h, 15cm, 22 kV, and (G) gelatin/tannic acid (20%/3%w/w) 0.8mL/h, 15cm, 25 kV

Higher entanglement of the polymer chain results in higher viscosity value³⁰. The capillary breakup of the spinning jet by surface tension is the main reason for the formation of droplets on the collector.

The changes in viscosity as a function of the shear rate for different spinning solutions are depicted in Fig. 2. It is clear that for all samples, the apparent viscosity remains nearly constant with increasing shear rates, indicating the Newtonian fluid-like behavior of the solutions. Such behavior for gelatin is already reported by various researchers³⁰. By increasing the tannic acid in the solution, the apparent viscosity is increased, which indicates the higher amounts of entanglement of polymer chains, due to the crosslinking role of tannic acid. The apparent viscosity for the gelatin (15%), gelatin (20%), gelatin/tannic acid (15%/3%), gelatin/tannic acid (15%/5%), gelatin/tannic acid (20%/3%) and gelatin/tannic acid (20%/5%) at the shear rate of 10^0 is found 0.68, 1.51, 1.47, 1.69, 2.11 and 2.69 Pa. S respectively.

From the SEM images, it is evident that the fibrous structure with uniform morphology is obtained from 20% gelatin solution. For the gelatin/tannic acid (15%/3%) and the gelatin/tannic acid (15%/5%) solutions at the voltage range of 20-25 kV, the feeding rate and distance are kept constant as 0.8 mL/h and

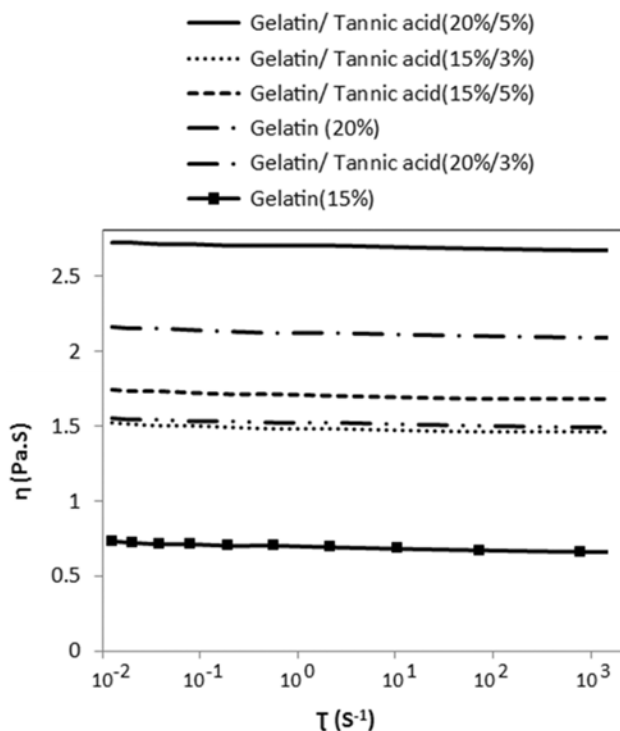


Fig. 2 — Changes of the viscosity as a function of the shear rate

15 cm, respectively. The effects of different electrospinning parameters on the gelatin morphology with the concentration of 20%w/w have previously been investigated³¹. In this regard, the morphology of tannic acid containing gelatin nanofibres is evaluated. For the gelatin/tannic acid (20%/3%), a beaded structure is observed, which is due to the high viscosity of the spinning solution (high voltage ranges 20-25 kV). The production ability of nanofibres for the gelatin/tannic acid (20%/5%) sample is non-existent, which can be attributed to the high solution viscosity. For the gelatin/tannic acid (20%/3%) sample, with increasing the applied voltage, the density of the beads decreased. It is reported that providing a balance between the electrostatic repulsion, surface tension and viscoelastic forces result in stabilization of the liquid jet and uniform morphology³⁰. It can be stated that applying the higher voltage to the liquid droplet can provide more appropriate conditions for producing nanofibres. Since the electrospinning process for producing nanofibres with bead-free morphology and uniform diameter is very important, the gelatin/tannic acid (15%/3%) and gelatin/tannic acid (15%/5%) are selected as optimum solutions and are used for further studies.

In the optimum concentration of gelatin/tannic acid, increasing the applied voltage causes an increase in the nanofibre diameter (Fig. 3). This can be due to the less branching of nanofibres in the spinning process³¹. The nanofibre diameter distribution for the optimum nanofibres is presented in Fig. 4.

As can be seen, the distribution of gelatin/tannic acid (15%/3%) nanofibres is broader than gelatin/tannic acid (15%/5%) nanofibres. It is concluded that the use of 5 % w/w tannic acid leads to production of nanofibres with more uniform morphology. The average nanofibre diameter for gelatin/tannic acid (15%/3%) and gelatin/tannic acid (15%/5%) at the high voltage of 22 kV is 103 and 108.1 nm respectively (feeding rate 0.8 mL/h and distance 15 cm). Increasing the tannic acid content in the spinning solution increased the average diameter value, due to the higher viscosity of the spinning solution¹⁸.

The effect of feeding rate of polymer in the spinning process is investigated and the results at different magnifications are shown in Fig. 5. It is found that the fibrous structure is not formed at the

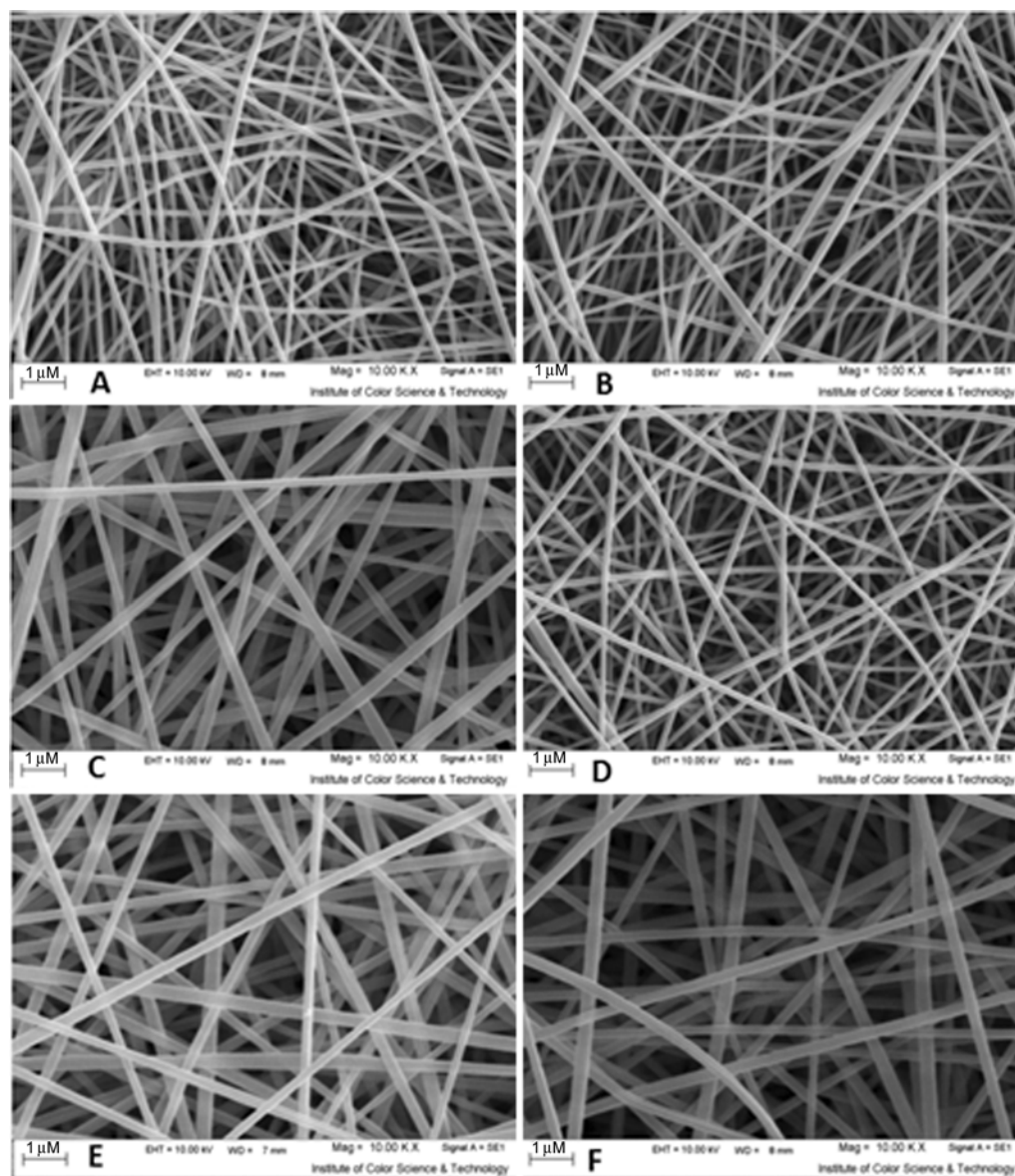


Fig. 3 — SEM images of optimum concentration of gelatin/tannic acid (A) 15%/3% w/w, 20 kV, (B) 15%/3% w/w, 22 kV, (C) 15%/3% w/w, 25 kV, (D) 15%/5% w/w, 20 kV, (E) 15%/5% w/w, 22 kV, and (F) 15%/5% w/w, 25 kV

feeding rate 0.4 mL/h. This can be due to the insufficient amount of solution in the spinneret. The nanofibres with uniform morphology are obtained when the feeding rate is kept 0.6 and 0.8 mL/h (distance 15 cm and high voltage 22 kV). The average diameter of gelatin/tannic acid (15%/3%) nanofibres is 98.2 and 103 nm for the feeding rate of 0.6 and 0.8 mL/h respectively. Moreover, the average diameter of gelatin/tannic acid (15%/5%) nanofibres is 100.6 and 108.1 nm for the feeding rate of 0.6 and 0.8 mL/h respectively. For this sample, increasing the feeding rate to 1 mL/h results in the formation of ribbon-like structure, due to the high amount of

injected polymer³². The ribbon-like structure is also observed at the distance of 12 cm and the feeding rate of 0.8 mL/h, on account of the incomplete evaporation of the solvent [Fig. 5(E)]. Additionally, the average width and diameter of gelatin/tannic acid (15%/5%) nanofibres at the feeding rate of 1 mL/h are 211.1 and 112 nm for the distances of 15 and 12 cm, respectively. For the gelatin/tannic acid (15%/5%), a beaded structure is observed at the distance of 12 cm and feeding rate of 1 mL/h.

The effect of feeding rate and distance on the morphology of gelatin/tannic acid (15%/3%) nanofibres are illustrated in Fig. 6. It is clear that all

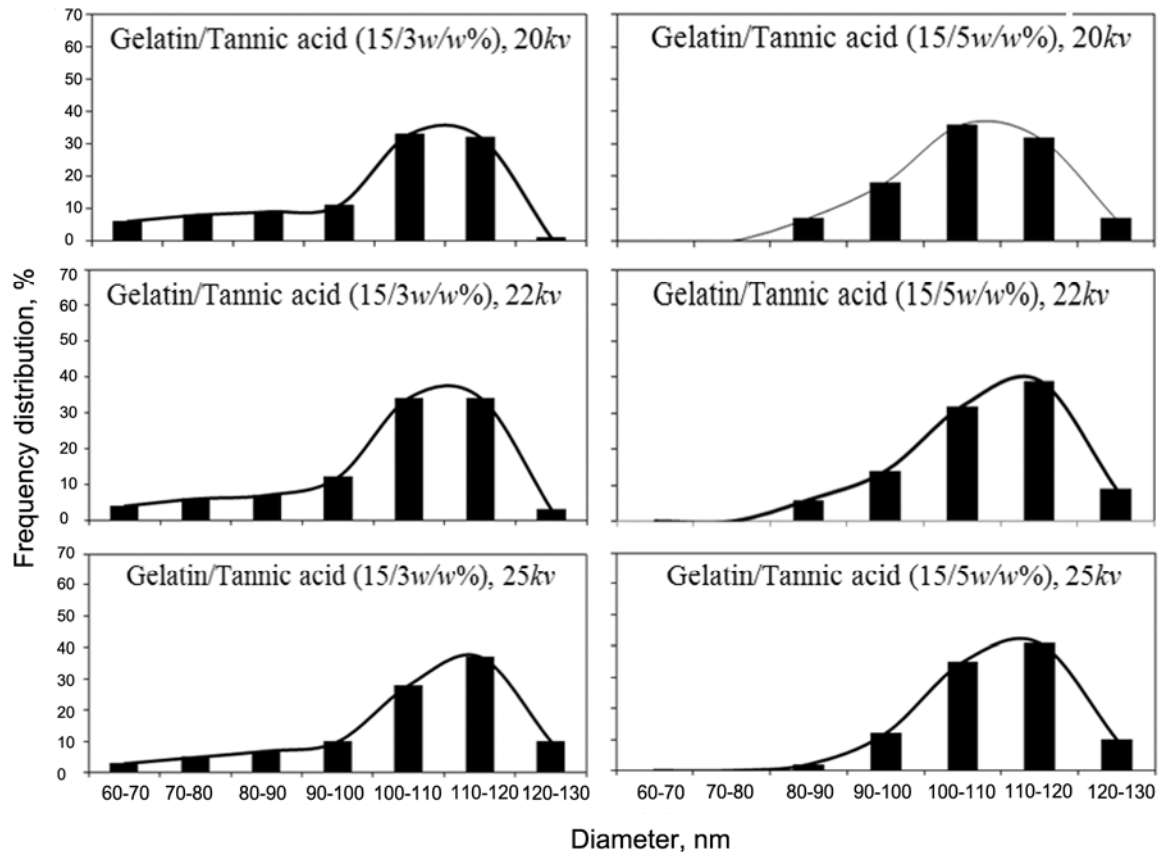


Fig. 4 — Distribution of nanofibre diameter for the optimum nanofibres

the samples show a bead free and uniform morphology. However, increasing the feeding rate lead to an increase in the average diameter of nanofibres. Moreover, decreasing the distance of the tip of the needle to the collector increases the average diameter of nanofibres. The average diameter of nanofibres produced at the distance of 15 cm and feeding rate of 0.6 mL/h is 98.2 nm, which increases to 104 nm when the distance is decreased to 12 cm.

3.2 Chemical Properties

The FTIR spectra of gelatin (20%) and gelatin/tannic acid (15%/5%) nanofibres are shown in Fig. 7(A). For the gelatin nanofibres, the appeared bands at 3452, 1668, 1540 and 1344 cm^{-1} are attributed to amide A, amide I, amide II and amide III respectively³³. Furthermore, the band related to the asymmetric stretching vibration of amide B is observed at 3048 cm^{-1} (ref. 34). The asymmetric and symmetric stretching vibrations of methylene groups in the glycine and proline are reflected at 2945 and 2885 cm^{-1} respectively²⁹. The band at 1249 cm^{-1} is

assigned to the combination peaks of C–N stretching vibrations and N–H deformation from amide linkages. Researchers have stated that the peak observed at around 1250 cm^{-1} is related to the asymmetric COC stretching vibrations³⁵. In the spectrum of gelatin/tannic acid (15%/5%) nanofibres, similar peaks to the spectrum of gelatin nanofibres are observed, although with some changes in their wavenumbers. The bands at 3452 and 1668 cm^{-1} are shifted towards the 3389 and 1698 cm^{-1} respectively, which can be an indication of differences in hydrogen bonding and protein conformation³⁴. It is reported that when the N–H group of a peptide is involved in an H-bond; the position shifts towards lower wavenumbers³⁶. The band related to the stretching vibration of =C–H is overlapped with the asymmetric stretching vibration of amide B. The appeared band at 1498 cm^{-1} is attributed to the stretching vibration of C–C in aromatic rings of tannic acid³⁷. From the result of FTIR analysis, it can be concluded that the tannic acid interacts with gelatin polymer through the hydrogen bonds.

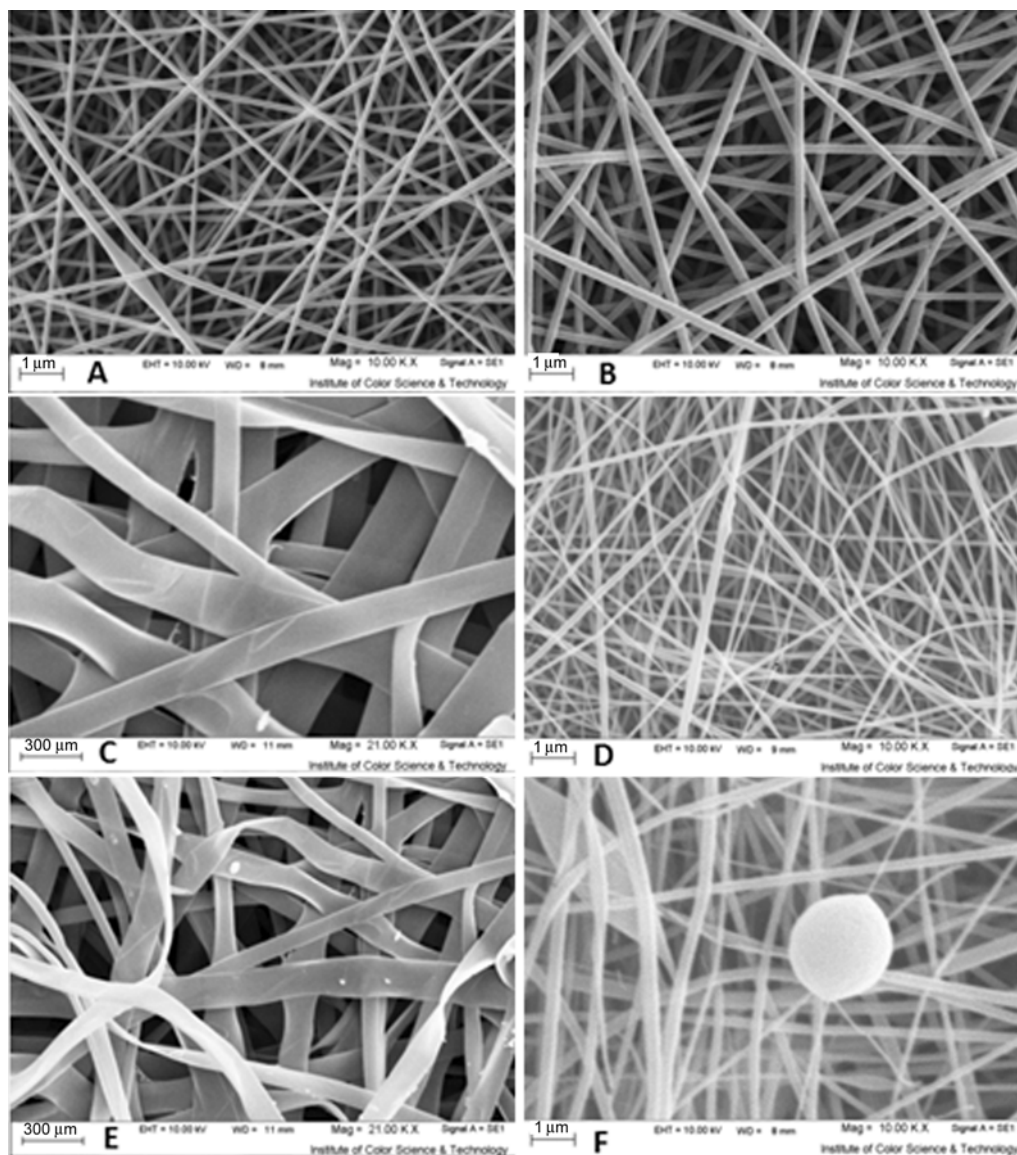


Fig. 5 — Effect of feeding rate of polymer in spinning process of gelatin/tannic acid (15/5%w/w): (A) 22kV- 15cm- 0.6 mL/h, (B) 22kV- 15cm- 0.8 mL/h, (C) 22kV- 15cm- 1 mL/h, (D) 22kV- 12cm- 0.6 mL/h, (E) 22kV - 12cm- 0.8 mL/h, and (F) 22kV- 12cm- 1 mL/h

Due to its unique amino acid sequences and numerous functional groups, gelatin is well-suited for producing chemical hydrogels in the form of sheets, films, or membranes by reacting with small molecules containing reactive functional groups, such as an aldehyde group^{24,38}.

In the mechanism of gelatin cross-linking, the reaction may have happened between free nonprotonated ϵ -amino groups ($-\text{NH}_2$) of lysine or hydroxylysine through a nucleophilic addition-type reaction²⁴. Therefore, between NH_2 and COOH groups, on the one hand in the gelatin structure, and OH in the acid tannic construction, on the other hand, crosslinking is formed by hydrogen bonding.

3.3 Mechanical Strength

Mechanical properties of gelatin (20%), gelatin/tannic acid (15%/3%) and gelatin/tannic acid (15%/5%) nanofibres are shown in Table 1. The results indicate that the tensile strength of tannic acid containing samples increases as compared to the gelatin nanofibres, due to crosslinking of polymeric chains. On the other hand, elongation-at-break of nanofibres decreases for the crosslinked nanofibres, which can be due to the restriction of polymeric chains movements. By increasing the amount of tannic acid, the tensile strength is increased and the elongation at break decreased.

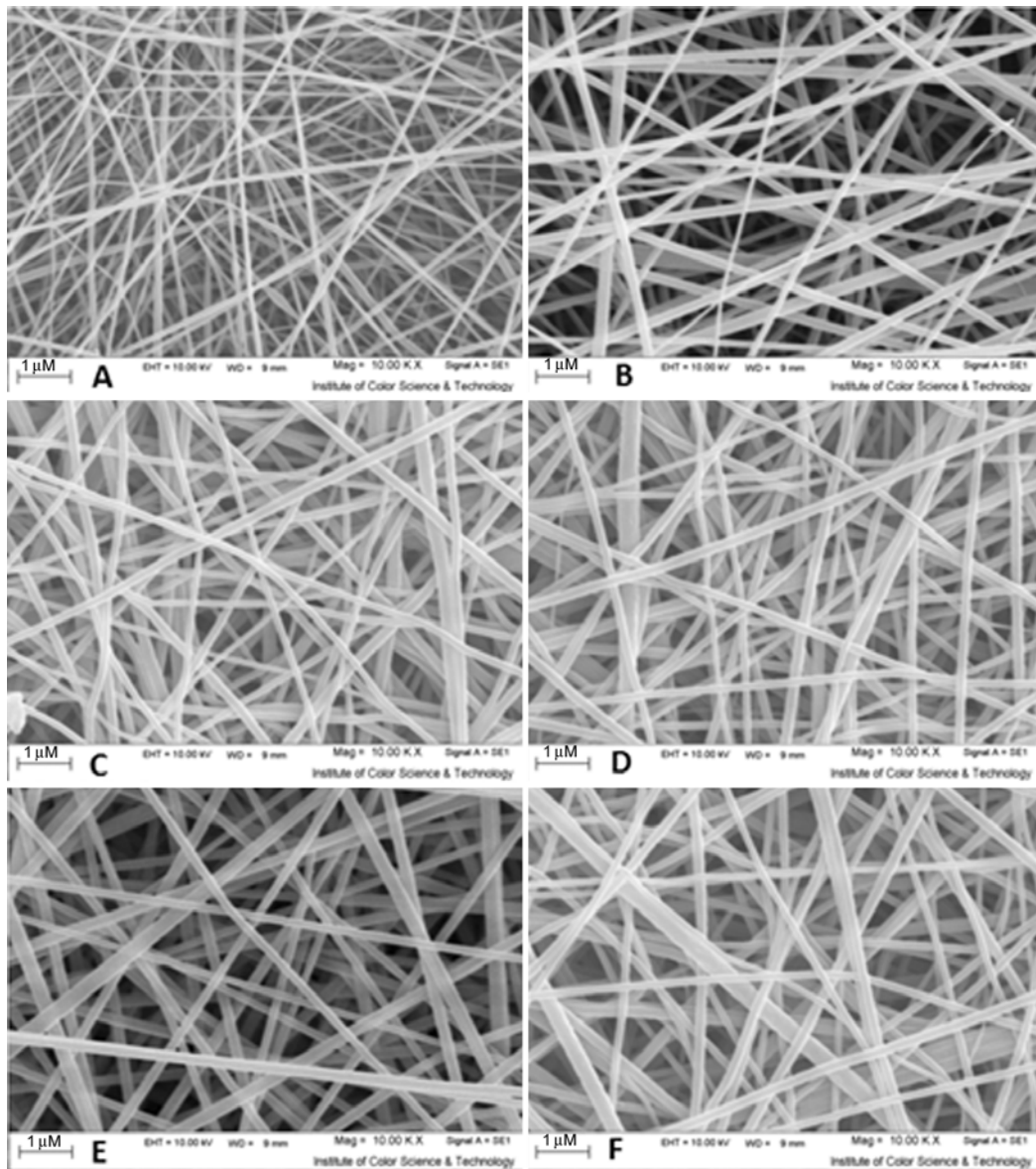


Fig. 6 — Effect of feeding rate and distance on the morphology of gelatin/tannic acid (15%/3%) nanofibres: (A) 22kV- 15cm- 0.6 mL/h, (B) 22kV- 15cm- 0.8 mL/h, (C) 22kV- 15cm- 1 mL/h, (D) 22kV- 12cm- 0.6 mL/h, (E) 22kV- 12cm- 0.8 mL/h, and (F) 22kV- 12cm- 1 mL/h

3.4 TGA Analysis

Thermal gravimetric analysis (TGA) for gelatin (20%), gelatin/tannic acid (15%/3%) and gelatin/tannic acid (15%/5%) nanofibres is performed and the results are shown in Fig. 7(B). It is clear that the gelatin nanofibres show a weight loss of 16% in the temperature range 30-110°C. The weight loss in this region is due to the removal of the physically adsorbed water molecules³⁹. The TGA curve shows a significant weight loss (42.5%) in the temperature range 110-250°C, which is due to the removal of chemisorbed water and degradation of polymeric chains⁴⁰. The change in this region is also related to

the loss of glycerol compound⁴¹. The weight loss at the higher temperature of 250°C is attributed to the loss of high molecular weight protein fractions⁴². For the gelatin/tannic acid (15%/5%) nanofibres, the weight loss decreases to 13.2% and 27.3% for the temperature range 30°-110°C and 110°-250°C respectively. Additionally, the weight loss for the gelatin/tannic acid (15%/3%) is 14.25 and 32.95 % respectively, indicating the higher thermal resistance of gelatin/tannic acid nanofibres due to the crosslinking role of tannic acid. The result of TGA analysis is in agreement with the results of FTIR analysis.

3.5 Contact Angle Analysis

The wettability of gelatin/tannic acid nanofibres is investigated by contact angle analysis. The results [Fig. 7(C)] show that the water droplet has a contact angle of 46° for the gelatin, 22.1° for the gelatin/tannic acid (15%/3%) and 30.1° for the gelatin/tannic acid (15%/5%) nanofibres, respectively, indicating the hydrophilic nature of nanofibres. Like other protein polymers, gelatin contains amine and carboxylic groups, which is the characteristic of a hydrophilic compound¹⁴. The hydrophilicity of nanofibres slightly decreases, since the polymeric chains of gelatin are cross linked together by tannic acid. Moreover, the presence of aromatic rings can be another reason for the decrease in the hydrophilicity of nanofibres.

3.6 Solubility and Water Absorbency

The results of nanofibre solubility show that the gelatin nanofibres completely solubilize after immersing in distilled water. The gelatin/tannic acid

(15%/3%) nanofibres show 14.65% weight loss. For the sample containing 5% w/w tannic acid, no weight loss is observed, indicating the fully crosslinked structure of nanofibres. Due to the solubility of gelatin and gelatin/tannic acid (15%/3%) nanofibres, they are not used for investigating the water absorbency. The water absorption capacity of gelatin/tannic acid (15%/5%) nanofibres is 12.59 mg/g. The high water absorption capacity of nanofibres can be attributed to the high amounts of hydrophilic groups in the gelatin structure.

3.7 Antibacterial Properties of Nanofibres

The antibacterial activity of gelatin and gelatin/tannic acid nanofibres is tested using the viable cell-counting method, and the results are shown in [Fig. 7(D)]. As can be seen, the gelatin nanofibres show no activity against the tested bacteria. *E. coli* (Gram-negative) is one of the common microorganisms that can be selected for antimicrobial tests and is resistant to common antimi-

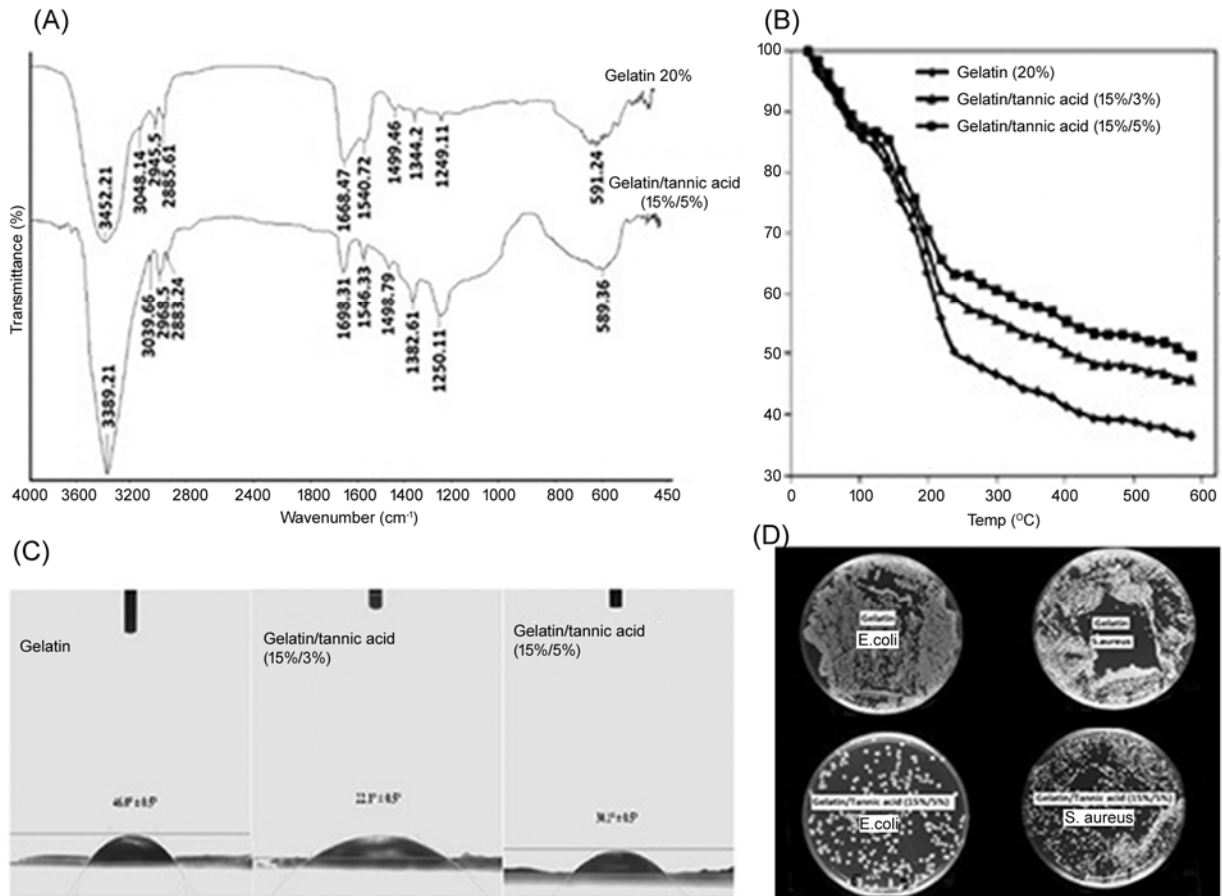


Fig. 7 — (A) FTIR spectra of gelatin (20%) and gelatin/tannic acid (15%/5%) nanofibres. (B) thermal gravimetric analysis for gelatin (20%), gelatin/tannic acid (15%/3%) and gelatin/tannic acid (15%/5%) nanofibers and (C and D) water contact angle and antibacterial activities of nanofibres

Table 1 — properties of gelatin (20%), gelatin/tannic acid (15%/3%) and gelatin/tannic acid (15%/5%) nanofibres

Nanofibres	Gelatin (20%)	Gelatin/tannic acid (15%/3%)	Gelatin/tannic acid (15%/5%)
Tensile strength, MPa	17.9	22.64	29.83
Elongation at break, %	12.88	10.05	8.87

crobial agents and *S. aureus* (Gram positive) bacteria is a major cause of disease in a hygienic environment⁴³. antibacterial efficiency of nanofibres increases to 48.89 and 63.52% for *S. aureus* and *E. coli* respectively, after the addition of 5% w/w tannic acid. The antibacterial property of tannic acid is mainly related to the galloyl group (3,4,5-trihydroxyphenyl group)²⁷. Furthermore, the ability to inactivate microbial adhesions, enzymes, cell envelope transport proteins, and mineral uptake are the other reasons for the antibacterial property of tannic acid⁴⁴. On the other hand, the antibacterial activity of gelatin/tannic acid nanofibres against *E. coli* bacteria is higher than that of *S. aureus*. This can be related to the differences in cell surface structures of Gram-negative and Gram-positive bacteria. It is reported that the outer cell membrane of Gram-negative bacteria consists of lipopolysaccharide, which can be stabilized by divalent cations such as Mg^{2+} and Ca^{2+} ions⁴⁵. Tannic acid chelates with these cations and destabilizes the lipopolysaccharide cell surface layer of Gram-negative bacteria, and finally cytotoxicity occurs. Gram-positive bacteria have a thick peptidoglycan layer which can act as a preventive barrier against tannic acid.

4 Conclusion

In this study, crosslinked gelatin nanofibres are prepared by electrospinning technique. Tannic acid with antioxidant and antibacterial properties is used as the crosslinking agent. The addition of tannic acid to the gelatin spinning solution increases the viscosity of the solution and limited the spinning process. It is observed that the blended solution with the tannic acid concentration of 5% w/w is crosslinked the gelatin chains completely (the concentration of gelatin solution was 15% w/w). The crosslinked nanofibres has the water absorption capacity of 12.59 mg/g. An investigation on the effects of electrospinning parameters on the nanofibre morphology reveals that increasing the feeding rate and high voltage values results in higher average nanofibre diameter. The

gelatin/tannic acid (15%/3%) and gelatin/tannic acid (15%/5%) nanofibres show a uniform morphology at the voltage range of 20-25 kV, feeding rate of 0.6-0.8 mL/h and the distance of 15 cm. The prepared nanofibres has the antibacterial activity of 48.89% and 63.52% against the *S. aureus* and *E. coli* bacteria, respectively. It is suggested that the produced nanofibres can be used as scaffolds in tissue engineering aspects.

References

- Gu S-Y, Wang Z-M, Ren J & Zhang C-Y, *Mater Sci Eng C*, 29 (2009) 1822.
- Burg K J L, Porter S & Kellam J F, *Biomater*, 21 (2000) 2347.
- Ghasemi-Mobarakeh Lh, Prabhakaran M, Morshed M, Nasr-Esfahani M-H & Ramakrishna S, *Biomater*, 29 (2008) 4532.
- Bhardwaj N & Kundu S C, *Carbohydrate Polym*, 85 (2011) 325.
- Harrington W F & Von Hippel P H, *Adv Protein Chem*, 16 (1961) 1.
- Mindru T B, Mindru I B, Malutan T & Tura V, *J Optoelectronics Adv Mater*, 9 (2007) 3633.
- Chong E J, Phan T T, Lim I J, Zhang Y Z, Bay B H, Ramakrishna S & Lim C T, *Acta Biomaterialia*, 3 (2007) 321.
- Koh H S, Yong T, Chan C K & Ramakrishna S, *Biomater*, 29 (2008) 3574.
- Linh N T B & Lee B-T, *J Biomater Appl*, 27 (2012) 255.
- Deitzel J M, Kleinmeyer J, Harris D E A & Tan N C B, *Polym*, 42 (2001) 261.
- Zhang Y, Ouyang H, Lim C T, Ramakrishna S & Huang Z-M, *J Biomed Mater Res B*, 72 (2005) 156.
- Mao J, Zhao L, Yao K, Shang Q, Yang G & Cao Y, *J Biomed Mater Res A*, 64 (2003) 301.
- Liu H, Mao J, Yao K, Yang G, Cui L & Cao Y, *J Biomater Sci Polym*, 15 (2004) 25.
- Mao J S, Liu H F, Yin Y J & Yao K D, *Biomaterials*, 24 (2003) 1621.
- Ko J H, Yin H Y, An J & Chung D J, *Macromolecular Res*, 18 (2010) 137.
- [16]. Bigi A, Cojazzi G, Panzavolta S, Rubini K & Roveri N, *Biomaterials*, 22 (2001) 763.
- Ramakrishna S, Fujihara K, Teo W E, Yong T, Ma Z & Ramaseshan R, *Mater Today*, 9 (2006) 40.
- Andrady A L, *Science and Technology of Polymer Nanofibres* (John Wiley & Sons Inc.Pub.), (2008).
- Son W K, Youk J H, Lee T S & Park W H, *Polym*, 45 (2004) 2959.
- Farris S, Schaich K M, Liu L, Cooke P H, Piergiovanni L & Yam K L, *Food Hydrocolloids*, 25 (2011) 61.
- E.J.Chong, T.T.Phan, I.J.Lim, Y.Z.Zhang, B.H.Bay, S.Ramakrishna, C.T.Lim, *Acta Biomater*, 3 (2007) 321.
- Zhang Y Z, Venugopal J, Huang Z-M, Lim C T & Ramakrishna S, *Polym*, 47 (2006) 2911.
- Huang Z-M, Zhang Y Z, Ramakrishna S & Lim C T, *Polym*, 45 (2004) 5361.
- Ki C S, Baek D H, Gang K D, Lee K H, Um I C & Park Y H, *Polym*, 46 (2005) 5094.
- Zhang Y, Ouyang H, Lim C T, Ramakrishna S & Huang Z M, *J Biomed Mater Res B Appl Biomater*, 72 (2005) 156.

- 26 Toshitsugu T, Takashi T & Isao K, *Biological Pharmaceutical Bulletin*, 27 (2004) 1965.
- 27 Kim T J, Silva J L & Jung Y S, *Food Chem*, 126 (2011) 116.
- 28 Zhang M, Cheng Z, Zhao T, Liu M, Hu M & Li J, *Agric Food Chem J*, 62 (2014) 8867.
- 29 Matabola K P & Moutloali R M, *Mater Sci J*, 48 (2013) 5475.
- 30 Almasian A, Mahmoodi N M & Olya M E, *Indus Eng Chem*, 32 (2015) 85.
- 31 Gomez-Mascaraque L G, Lagaron J Ma & Lopez-Rubio A, *Food Hydrocolloids*, 49 (2015) 42.
- 32 Okutan N, Terzi P & Altay F, *Food Hydrocolloids*, 39 (2014) 19.
- 33 Son W K, Youk J H, Lee T S & Park W H, *Polym*, 45 (2004) 2959.
- 34 Meng Li, Klinkajon W, K-hasuwan P, Harkin S, Supaphol P & EWnek G, *Polym Int*, 64 (2015) 42.
- 35 Almasian A, Najafi F, Mirjalili M, Gashti M P & Fard G C, *J Taiwan Inst Chem Eng*, 67 (2016) 306.
- 36 Muralidharan N, Sootawat B, Thummanoon P, Ponusa S & Pornpot N, *Food Chem*, 138 (2013) 1101.
- 37 Catledge S A, Clem W C, Shrikishen N, Chowdhury S, Stanishevsky A V, Koopman M & Vohra YK, *Biomedical Mater*, 2 (2007) 142.
- 38 Almasian A, Jalali M L, Fard G C & Maleknia L, *Chem Eng J*, 326 (2017) 1232.
- 39 Gashti M P & Almasian A, *Composites: Part B*, 43 (2012) 3374.
- 40 Gashti M P & Almasian A, *Composites: Part B*, 52 (2013) 340.
- 41 Ahmad M, Benjakul S, Prodpran T & Agustini T W, *Food Hydrocolloids*, 28 (2012) 189.
- 42 Hoque M S, Benjakul S & Prodpran T, *Food Chem*, 128 (2011) 878.
- 43 Challa S S R Kumar, *Tissue, Cell and Organ Eng* (Wiley-Vch Verlag GmbH & Co. KGaA, Weinheim), 2006, 159.
- 44 Chung K T, Wong T Y, Wei C I, Huang Y W & Lin Y, *Critical Rev Food Sci Nutrition*, 38 (1998) 421.
- 45 Pyla R, Kim T-J, Silva J L & Jung Y-S, *Int J Food Microbiol*, 137 (2010) 154.